

## Thermodynamic properties of oxygen in RE–O (RE=Gd, Tb, Dy, Er) solid solutions

T.H. Okabe\*, K. Hirota<sup>1</sup>, E. Kasai, F. Saito, Y. Waseda, K.T. Jacob<sup>2</sup>

*Institute for Advanced Materials Processing, Tohoku University, Sendai 980-8577, Japan*

Received 29 May 1998

---

### Abstract

The oxygen potentials of four rare-earth metal – oxygen (RE–O: RE=Gd, Dy, Tb, Er) solid solutions have been measured by equilibration with yttrium – oxygen (Y–O) and titanium – oxygen (Ti–O) solid solutions. Rare-earth metal, yttrium and titanium samples were immersed in calcium-saturated  $\text{CaCl}_2$  melt at temperatures between 1093 and 1233 K. Homogeneous oxygen potential was established in the metallic samples through the fused salt, which contains some dissolved CaO. The metallic samples were analyzed for oxygen after quenching. The oxygen potentials of RE–O solid solutions were determined using either Y–O or Ti–O solid solution as the reference. This method enabled reliable measurement of extremely low oxygen potentials at high temperature (circa  $p_{\text{O}_2} = 10^{-48}$  atm at 1173 K). It was found that the oxygen affinity of the metals decreases in the order:  $\text{Y} > \text{Er} > \text{Dy} > \text{Tb} > \text{Gd} > \text{Ti}$ . Values for the standard Gibbs energy of solution of oxygen in RE metals obtained in this study, permit assessment of the extent of deoxidation that can be achieved with various purification techniques. It may be possible to achieve an oxygen level of 10 mass ppm using an electrochemical deoxidation method. © 1998 Elsevier Science S.A. All rights reserved.

**Keywords:** Rare-earth metals; Gadolinium; Terbium; Dysprosium; Erbium; Yttrium; Solution of oxygen; Thermodynamics; Gibbs energy; Deoxidation

---

### 1. Introduction

For many new applications of rare-earth (RE) metals, materials of high purity are required [1,2]. In parallel with efforts for the production of metals of purity greater than 99.999% (excluding carbon and gaseous elements) for use in electronics [3], the importance of thermodynamic data for main impurity elements in RE metals has been well recognized. Although metallic impurities in RE metals can be kept at a fairly low level, a major impurity in these materials is oxygen, present in amounts varying from 0.05 to 1 wt % (500 to 10 000 ppm). Generally, oxygen removal from RE metals is very difficult because of their strong affinity and high solubility for oxygen [4–7]. There is no

specific information in the literature on the activity and solubility of oxygen in heavy RE metals.

Recently, electrochemical deoxidation has been used for removing oxygen from titanium and titanium aluminides [8–10]. Titanium containing less than 10 mass ppm oxygen, which is below the detection limit of conventional gas analysis [11], has been produced by the electrochemical technique. The method has also been applied for oxygen removal from yttrium–oxygen (Y–O) solid solution [12]; yttrium metal containing 5700 mass ppm oxygen was directly deoxidized below 100 ppm level.

Reported in this article is the development of a method for measuring extremely low oxygen chemical potentials of the order of  $-1000 \text{ kJ mol}^{-1}$  at 1150 K, which is far beyond the range of applicability of oxide solid electrolytes and gas-equilibration techniques. The method is used for measuring the oxygen potentials of heavy rare-earth metals (RE=Gd, Tb, Dy, Er) containing dissolved oxygen. Information on oxygen chemical potentials in RE–O solid solutions can be utilized not only for estimating the limit of deoxidation but also for the optimization of process parameters in the production of high purity RE metals.

---

\*Corresponding author.

<sup>1</sup>Present address: Shin-Etsu Chemical Co. Ltd., Kitago 2-chome, Takefu-city, Fukui, Japan 915-8515.

<sup>2</sup>On sabbatical leave from Department of Metallurgy, Indian Institute of Science, Bangalore, India.

## 2. Principle of the ultra-low oxygen potential measurement

Ultra-low oxygen potentials of RE–O solid solutions were measured by an indirect technique involving equilibration of RE–O specimens with Y–O or Ti–O solid solutions, which act as reference materials. These reference solutions were employed because their thermodynamic properties are known [13–17]. A diagrammatic summary of the data for the reference solutions is presented in Fig. 1 in comparison with data for selected metal–oxide couples. More specifically, the Gibbs energy of solution of oxygen, which provides the relationship between oxygen content, [O], and oxygen partial pressure,  $p_{O_2}$ , is known as a function of temperature. Within the accuracy of measurement, the reference solutions were found to obey Sievert's law.

The Gibbs energy change associated with the solution of oxygen in RE metals,  $\Delta G_1^\circ$ , can be represented as follows:

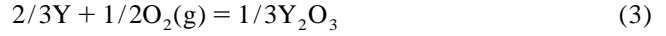


$$\Delta G_1^\circ = -RT \ln(f_{O(RE)} \cdot [wt \% O]_{RE} / p_{O_2}^{1/2}) \quad (2)$$

where  $[wt \% O]_{RE}$  is the equilibrium concentration of oxygen in wt % in RE metal at temperature  $T$  (K) and oxygen partial pressure  $p_{O_2}$  (atm),  $f_{O(RE)}$  is the Henrian activity coefficient of oxygen in solution, expressed relative to an infinitely dilute solution of oxygen in the RE

metal in which activity of the solute is equal to its concentration in wt %. When Sievert's law is obeyed by dissolved oxygen, value of the Henrian activity coefficient is unity. By measuring  $[wt \% O]_{RE}$  at equilibrium under known values of  $p_{O_2}$  in the ambient atmosphere at various temperatures,  $\Delta G_1^\circ$  can be evaluated as a function of  $T$ .

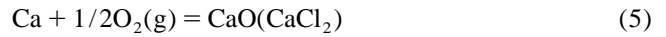
In the present study, the oxygen partial pressure is fixed using two methods. In the first method, a two-phase mixture of a metal and its oxide controls the oxygen partial pressure. For example, the  $p_{O_2}$  established by Y/Y<sub>2</sub>O<sub>3</sub> equilibrium can be expressed by the equations:



$$\Delta G_{f(Y_2O_3)}^\circ = -RT \ln(a_{Y_2O_3}^{1/3} / a_Y^{2/3} \cdot p_{O_2}^{1/2}) \quad (4)$$

where  $\Delta G_{f(Y_2O_3)}^\circ$  is the standard Gibbs energy of formation of Y<sub>2</sub>O<sub>3</sub>, and  $a_i$  is activity of species  $i$ . Among the different metal/metal-oxide buffers, Y/Y<sub>2</sub>O<sub>3</sub> equilibrium has the lowest  $p_{O_2}$ . The  $p_{O_2}$  can be calculated directly from the literature value for  $\Delta G_{f(Y_2O_3)}^\circ$  when the metal and oxide are at unit activity.

The second method for controlling oxygen partial pressure at very low values employs calcium-saturated CaCl<sub>2</sub> molten salt with a small amount of dissolved CaO. The  $p_{O_2}$  varies with the concentration of CaO dissolved in the fused salt. The equilibrium controlling the  $p_{O_2}$  can be represented as:



$$\Delta G_{f,CaO}^\circ = -RT \ln(a_{CaO} / a_{Ca} \cdot p_{O_2}^{1/2}) \quad (6)$$

The activity of Ca ( $a_{Ca}$ ) in Ca-saturated CaCl<sub>2</sub> is close to unity. When the activity of CaO ( $a_{CaO}$ ) in CaCl<sub>2</sub> is high,  $p_{O_2}$  defined by Eq. (5) exceeds the value corresponding to the Y/Y<sub>2</sub>O<sub>3</sub> equilibrium [13], because the standard Gibbs energy of formation of CaO is more positive than that of Y<sub>2</sub>O<sub>3</sub> per mole of oxygen. By using CaCl<sub>2</sub> containing low concentration of oxygen (CaO),  $p_{O_2}$  can be established at lower values. The  $p_{O_2}$  in the calcium-saturated CaCl<sub>2</sub> molten salt can be determined by measuring oxygen content of the reference materials, such as titanium or yttrium metal in equilibrium with the salt. The Gibbs energy change associated with the dissolution of oxygen in yttrium and titanium, available in the literature [13,17], can be expressed as follows:



$$\Delta G_7^\circ = -RT \ln(f_{O(Y)} \cdot [wt \% O]_Y / p_{O_2}^{1/2}) \quad (8)$$



$$\Delta G_9^\circ = -RT \ln(f_{O(Ti)} \cdot [wt \% O]_{Ti} / p_{O_2}^{1/2}) \quad (10)$$

By combining Eq. (2) and (8), one obtains:

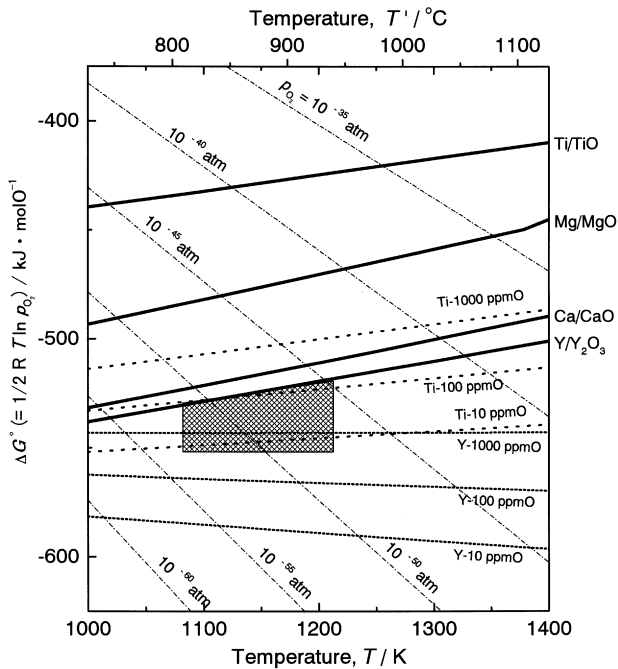


Fig. 1. Ellingham diagram for selected oxides and Ti–O and Y–O solid solutions. The range of oxygen potentials measured in this study is depicted by the cross-hatched region

$$\Delta G_1^\circ = \Delta G_7^\circ - RT \ln(f_{O(RE)} \cdot [\text{wt \% O}]_{RE} / f_{O(Y)} \cdot [\text{wt \% O}]_Y) \quad (11)$$

The standard Gibbs energy change for reaction (1),  $\Delta G_1^\circ$ , can be determined from the value of  $\Delta G_7^\circ$  and the distribution coefficient of oxygen between RE and Y,  $K_{RE/Y} = [\text{wt \% O}]_{RE} / [\text{wt \% O}]_Y$ , when Sievert's law is obeyed by oxygen in RE and Y. The value of  $\Delta G_1^\circ$  so obtained can be cross-checked using distribution coefficient of oxygen between RE and Ti,  $K_{RE/Ti} = [\text{wt \% O}]_{RE} / [\text{wt \% O}]_{Ti}$ :

$$\Delta G_1^\circ = \Delta G_9^\circ - RT \ln K_{RE/Ti} \quad (12)$$

### 3. Experimental aspects

Table 1 shows the oxygen and nitrogen content of metal samples used in this investigation. Reagent grade anhydrous  $\text{CaCl}_2$  powder was dried under vacuum at 500 K for 7 days prior to use.

A schematic diagram of the apparatus used for equilibration is shown in Fig. 2. Five to ten pieces of rare earth metals, yttrium and titanium were placed in a titanium cup filled with  $\text{CaCl}_2$ . The different metals were separated from each another by means of titanium foil. The titanium cup containing the metallic samples and  $\text{CaCl}_2$  was sealed in an outer stainless steel vessel with an excess of calcium metal. To avoid contamination of the samples by impurities – mainly oxygen and nitrogen – in metallic calcium, calcium metal was physically isolated from the fused salt. Calcium was supplied to the  $\text{CaCl}_2$  melt via the vapor phase. The  $\text{CaCl}_2$  melt acted as an oxygen reservoir in which oxygen potential was maintained at a constant value. The oxygen potential was defined by  $\text{Ca}/\text{CaO}$  equilibrium, where the activity of  $\text{CaO}$  is maintained at a low value. In another experimental setup, a mixture of yttrium metal turnings and yttria ( $\text{Y}_2\text{O}_3$ ) powder were placed in the titanium cup along with  $\text{CaCl}_2$  to set the

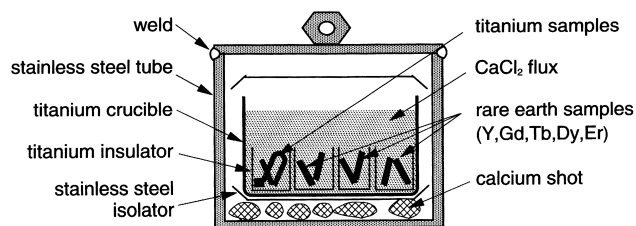


Fig. 2. Reaction vessel used for the measurement of ultra-low oxygen potentials.

oxygen potential at a value corresponding to  $\text{Y}/\text{Y}_2\text{O}_3$  equilibrium.

The sealed stainless steel vessel was heated in an electric furnace to a temperature between 1093 and 1233 K. Experimental conditions are given in Table 2. The holding time was between 260 ks (3 days) and 1210 ks (14 days), after which the vessel was quenched in water. The holding time for attaining equilibrium concentrations of oxygen in metal samples was selected from previous studies on the  $\text{Y}-\text{O}$  [13] and  $\text{Ti}-\text{O}$  [16] systems. The diffusion coefficient of oxygen in yttrium and gadolinium is larger than that in titanium [18].

After quenching the reaction vessel to room temperature, calcium-saturated fused salt in the titanium cup was mechanically removed, and the rare earth and titanium samples were collected. The rare earth samples were cleaned in water, and mechanically polished. The titanium samples were cleaned in water, alcohol and acetone, and then allowed to dry.

Oxygen and nitrogen concentrations were determined by an inert gas fusion-infrared absorption method (LECO TC-436 analyzer). Prior to the oxygen and nitrogen analyses, the samples were again mechanically polished, and the titanium samples were chemically etched with a 1:4:10 mixture of  $\text{HF}:\text{HNO}_3:\text{H}_2\text{O}$ . For oxygen and nitrogen extraction, 0.1 g of sample enclosed in 1 g of platinum or nickel foil was dropped into a graphite crucible and heated to a temperature above 2000 K. The average blank

Table 1  
Analytical values of oxygen and nitrogen in titanium, yttrium and rare earth metal samples used in this study

Samples	Grade <sup>a</sup> (%)	Oxygen concentration, $C_{O(RE,Ti)}$ (mass ppm)	Nitrogen concentration, $C_{N(RE,Ti)}$ (mass ppm)	Configuration
Gadolinium	99.9 <sup>b</sup>	200	20	0.5 to 1.5 g/small pieces
Terbium	99.9 <sup>b</sup>	540	430	0.5 to 1.5 g/small pieces
Dysprosium	99.9 <sup>b</sup>	590	70	0.5 to 1.5 g/small pieces
Erbium	99.9 <sup>b</sup>	1500	160	0.5 to 1.5 g/small pieces
Yttrium	99.9 <sup>b</sup>	9700	250	0.5 to 1.0 g/small pieces
Titanium-1	99.999 <sup>c</sup>	210	10	0.1 to 0.2 g/small pieces
Titanium-2	99.9 <sup>b</sup>	950	20	1.1 mm diameter wire
Titanium-3	99.9 <sup>b</sup>	670	30	1.9 mm diameter wire

<sup>a</sup> Excluding gaseous elements.

<sup>b</sup> Commercial grade.

<sup>c</sup> Electron-beam melted, semiconductor-grade, high-purity sponge.

Table 2  
Conditions of equilibration

Exp. No.	Temp. [K]	Holding time [ks]	Equilibrium	Mass [g]			
				CaCl <sub>2</sub>	Ca	Y	Y <sub>2</sub> O <sub>3</sub>
A	1233	259	Ca/CaO in CaCl <sub>2</sub> ( $a_{\text{CaO}} < 1$ )	350	19.0	-	-
B	1118	691		350	21.7	-	-
C	1161	605		350	6.7	-	-
D	1137	605		350	2.0	-	-
E	1173	346		350	4.2	-	-
F	1093	691		350	4.6	-	-
X	1114	893	Y/Y <sub>2</sub> O <sub>3</sub> (without Ca)	350	-	3.22	1.33
V	1123	817		350	-	5.09	2.51
U	1213	551		350	-	5.66	2.56
T	1173	518		350	-	4.92	2.43
S	1093	1210		350	-	3.45	1.69
Z	1129	691	Y/Y <sub>2</sub> O <sub>3</sub> (with Ca)	350	6.8	2.94	1.49
Y	1173	432		350	6.1	3.11	1.45
W	1173	605		350	2.0	5.49	2.49

values of oxygen and nitrogen during analysis were 3.0 ( $\pm 1.0$ )  $\mu\text{g}$  and 0.5 ( $\pm 0.2$ )  $\mu\text{g}$ , respectively. The concentration of calcium and other metal impurities in the samples was determined by X-ray fluorescence analysis (XRF, Rigaku 3270) and by inductively coupled plasma – atomic emission spectrometry (SEIKO SPS-1200A).

#### 4. Results

The measured oxygen concentrations of metal samples equilibrated with calcium-saturated CaCl<sub>2</sub> melt containing dissolved CaO are summarized in Table 3. The oxygen concentration in all samples is found to decrease during equilibration with the molten salt. This confirms the ability

of calcium-saturated CaCl<sub>2</sub>, with low concentration of dissolved CaO, to establish very low oxygen chemical potentials.

The nitrogen concentration of RE metal samples increased during the high temperature experiment from the initial value by about 100 to 300 mass ppm. For titanium the increase was 50 to 100 mass ppm. Calcium concentration in the rare earth samples was unchanged from its initial value ( $\sim 150$  ppm), except for Gd where the concentration increased to 500 ppm after equilibration.

The oxygen concentration of the metal samples equilibrated with Y/Y<sub>2</sub>O<sub>3</sub> via molten CaCl<sub>2</sub> are summarized in Table 4. In the experiments without the addition of calcium metal to CaCl<sub>2</sub>, the oxygen concentration of yttrium is found to be close to the solubility limit [6], and oxygen

Table 3  
Oxygen concentration of titanium, yttrium and rare-earth metal samples equilibrated with calcium-saturated CaCl<sub>2</sub>; the  $p_{\text{O}_2}$  is fixed by Ca/CaO in CaCl<sub>2</sub> ( $a_{\text{CaO}} \ll 1$ )

Sample	Oxygen concentration, C <sub>O</sub> (mass ppm)						
	Initial	After equilibration with Ca/CaO in CaCl <sub>2</sub> ( $a_{\text{CaO}} \ll 1$ )					
		Exp. A 1233 K 259 ks	Exp. E 1173 K 346 ks	Exp. C 1161 K 605 ks	Exp. D 1137 K 605 ks	Exp. B 1118 K 691 ks	Exp. F 1093 K 691 ks
Gd	200	100, 110, 110, 120	100, 110	120, 120	120, 250	110, 170	130
Tb	540	210	–	340	160, 160, 190, 200	140	100, 120
Dy	590	200, 210, 210	190, 250, 250	180	140, 160, 190	180	160, 170
Er	1500	330, 420, 500	370, 380, 380	300	260, 290, 300	170	340, 350
Y	9700	3370, 3470	3120, 3300	2350, 2490	2060, 2100, 2210	1150, 1520	3220, 3260
Ti-1	210	40, 60	30, 50	140, 170	170, 170	160, 210	210, 230
Ti-2	950	10, 50	40, 60	50	220, 240	430, 440	900, 660
Ti-3	670	20, 40	40, 60	80, 150	420, 440	380, 390	640, 540

Table 4

Equilibrium oxygen concentration of titanium, yttrium and rare-earth metal samples equilibrated with  $Y/Y_2O_3$ 

Sample	Oxygen concentration, $C_O$ (mass ppm)								
	Initial	After equilibration with $Y/Y_2O_3$							
		Without calcium metal					With calcium metal		
		Exp. U 1213 K 551 ks	Exp. T 1173 K 518 ks	Exp. V 1123 K 807 ks	Exp. X 1114 K 892 ks	Exp. S 1093 K 1210 ks	Exp. Y 1173 K 432 ks	Exp. W 1173 K 604 ks	Exp. Z 1129 K 691 ks
Gd	200	480, 500	420, 450	290, 320	560, 710	240, 210	180, 200	260, 260	190, 240, 250
Tb	540	850, 890	1150, 1260	470, 470	840, 1240	660, 750	280, 280	410, 430	320, 320
Dy	590	–	1360, 1360	870, 950	820, 920	720, 730	440, 490	710, 720	360, 370
Er	1500	3390, 3320	7760, 9240	1750, 1800	1680, 1860	1720, 1650	930, 990	1670, 1770	670, 720
Y	9700	18 200, 18 300	15 000	11 600, 11 700	18 000, 25 200	15 100, 12 800	7600, 8100	13 600, 14 100	4700, 4700
Ti-1	210	90	40, 80	240, 290	340, 350	160, 210	60, 100	130, 180	170, 240
Ti-2	950	100, 220	160, 160	390, 410	540, 550	520, 530	320, 350	60, 90	–
Ti-3	670	80, 100	30, 240	400, 410	580, 320	470, 470	110, 160	60, 90	410, 430, 490

concentration of rare earth metals (Gd, Tb, Dy, and Er) falls in the range 200 to 2000 ppm. The results obtained with the addition of calcium metal to  $CaCl_2$  are also given in Table 4. The oxygen concentration of the metal samples is much lower when calcium metal is present in the reaction vessel. It is clear that the oxygen potential corresponding to  $Y/Y_2O_3$  equilibrium is not established in the vessel when calcium metal is present. In this case, there are two reactions (Eqs. (3) and (5)) competing for the control of oxygen potential in the fused salt. The  $Y/Y_2O_3$  equilibrium is essentially a heterogeneous reaction involving solid phases, whereas the  $Ca[CaCl_2]/CaO[CaCl_2]$  equilibrium occurs homogeneously in the fused salt because of the solubility of Ca and CaO in  $CaCl_2$ . Kinetics of the homogeneous reaction is probably more favorable than that of the heterogeneous reaction. Therefore, it is not surprising that the oxygen potential of the fused salt is controlled more by the homogeneous reaction occurring throughout the melt than by heterogeneous reaction at the interface of the  $Y/Y_2O_3$  mixture with the fused salt. The distribution ratios of oxygen,  $K_{RE/Ti}$  and  $K_{RE/Y}$ , obtained in the experiment with both  $Y/Y_2O_3$  and calcium present in the reaction vessel agree with the results from experiments in which only one oxygen buffer system is deployed. This indicates that the fused salt was able to establish the same oxygen potential around all the metallic samples immersed in it, except in the vicinity of the  $Y/Y_2O_3$  mixture.

The temperature dependence of saturation solubility of oxygen in yttrium and the corresponding equilibrium oxygen concentration in RE metals and titanium are displayed in Fig. 3. The diagram gives a visual impression of the reproducibility of oxygen determination at oxygen potentials defined by  $Y/Y_2O_3$  equilibrium. The oxygen concentration in titanium shows relatively large scatter because the values are close to the detection limit (about 10 mass ppm) of the analytical technique. Determination of

$p_{O_2}$  in the reaction vessel using Ti–O solid solutions in this low concentration range involves relatively large uncertainties. The values for saturation solubility of oxygen in yttrium obtained in this study is in good agreement with data reported by Carlson et al. [6]. At low oxygen potentials, the Y–O solid solution provides a better reference system than the Ti–O solid solution.

Shown in Fig. 4 is the relationship between the square root of  $p_{O_2}$  and dissolved oxygen concentration [O] in RE–O and Ti–O solid solutions at 1173 K. The values of

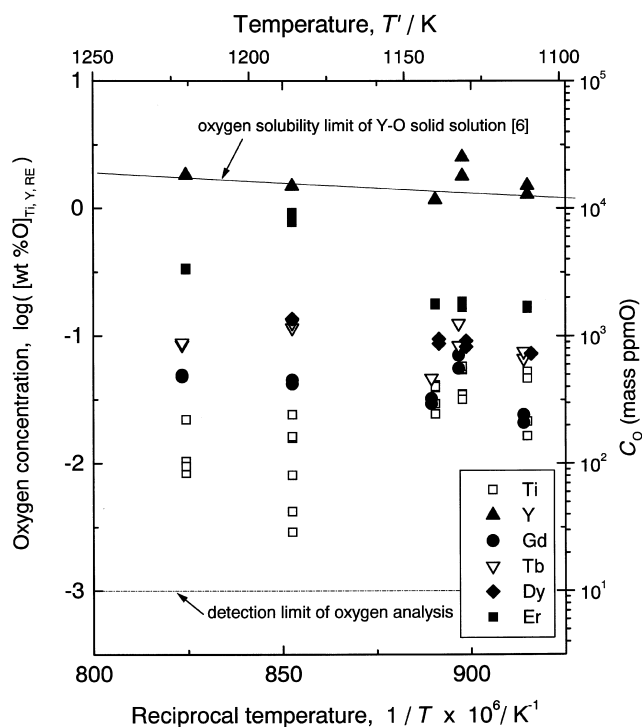


Fig. 3. Oxygen concentration in yttrium, RE metals and titanium after equilibration with  $Y/Y_2O_3$ , without addition of calcium to molten  $CaCl_2$ .

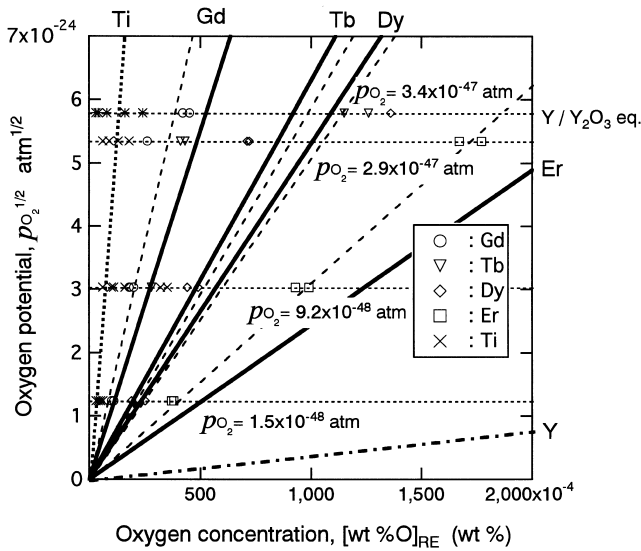


Fig. 4. Relationship between square root of oxygen partial pressure and oxygen concentration in RE–O (RE=Gd, Tb, Dy, Er), Y–O and Ti–O solid solutions at 1173 K. The dashed lines represents the mean value of Sievert's law constant obtained from the data shown on the diagram. The solid lines are obtained by regression analysis of data at all temperatures.

$p_{O_2}$  are calculated from the equilibrium oxygen concentration in the reference Y–O solid solution and the literature value of  $\Delta G_7^\circ$  [13]. The dashed lines are calculated from the data shown in the figure. The solid lines corresponds to equations for the Gibbs energy of solution of oxygen in RE metals obtained by least square regression analysis of all the data as a function of temperature, assuming Sievert's law (see Section 5). The difference in slope between the dashed and solid lines for each RE metal reflects the deviation of the Gibbs energy of solution of oxygen obtained from experiments at 1173 K from the regression equation. Although, the data suggest negative deviations from Sievert's law, especially for Tb, Dy and Er, the accuracy of measurement does not permit evaluation of the self-interaction parameter for oxygen. Only average values of the Sievert's law constant can be derived with confidence. The Sievert's law constants for the four heavy RE metals fall between values for titanium and yttrium.

The temperature dependence of the distribution coefficients of oxygen between RE metals and yttrium,  $K_{RE/Y} = [wt \%O]_{RE}/[wt \%O]_Y$ , is shown in Fig. 5. Values of  $RT \ln(K_{RE/Y})$ , which has same units as Gibbs energy, are plotted along the y-axis. Linear least-squares regression analysis of the data in Fig. 5 provides the following equations in the temperature range 1093 to 1223 K:

$$-RT \ln([wt \%O]_{Gd}/[wt \%O]_Y) = -19\,900 + 44.8T(\pm 5000)/J \text{ mol}^{-1} \quad (13)$$

$$-RT \ln([wt \%O]_{Tb}/[wt \%O]_Y) = 10\,900 + 13.9T(\pm 4200)/J \text{ mol}^{-1} \quad (14)$$

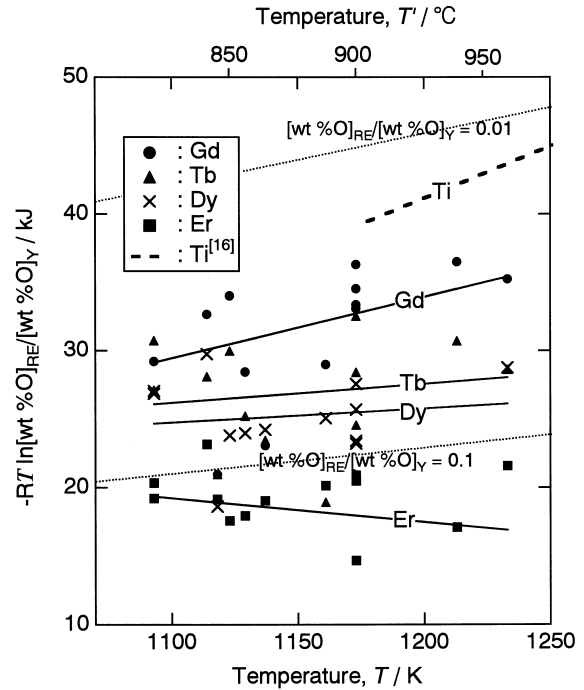


Fig. 5. Temperature dependence of the equilibrium distribution coefficients of oxygen between RE metal (RE=Gd, Tb, Dy, Er) and yttrium.

$$-RT \ln([wt \%O]_{Dy}/[wt \%O]_Y) = 13\,400 + 10.4T(\pm 3000)/J \text{ mol}^{-1} \quad (15)$$

$$-RT \ln([wt \%O]_{Er}/[wt \%O]_Y) = 38\,400 - 17.4T(\pm 3900)/J \text{ mol}^{-1} \quad (16)$$

Because of the scatter in the data shown in Fig. 5, these equations should not be extrapolated beyond the range of measurement. The slopes of the lines in Fig. 5 are rather uncertain. Separate terms in Eqs. (13) and (16) should not be interpreted in terms of relative enthalpies and entropies.

## 5. Discussion

The Gibbs energy change for the solution of oxygen in RE metals,  $\Delta G_1^\circ$ , can be determined from Eq. (13)–(16) and the value of  $\Delta G_7^\circ$  from the literature [13], assuming Sievert's law to be valid in the RE–O and Y–O systems;

$$\Delta G_1^\circ = \Delta G_7^\circ - RT \ln([wt \%O]_{RE}/[wt \%O]_Y) \quad (17)$$

The results are listed in Table 5 along with the reference data used for calculation. The calculated values of  $\Delta G_1^\circ$  are only valid within the investigated temperature range.

The Gibbs energy changes associated with the solution of diatomic oxygen gas,  $\Delta G_1^\circ$ , in the four RE metals are compared as a function of temperature with that for titanium in Fig. 6. Also plotted are the Gibbs energies of formation of sesquioxides of the corresponding RE metals,

Table 5

Summary of standard Gibbs energy changes associated with various reactions obtained in this study, together with auxiliary data for reference solutions

Reaction	Standard Gibbs energy change, J mol <sup>-1</sup>	Source
O (Y, 1 wt %) = O (Gd, 1 wt %) <sup>a</sup>	$\Delta G^\circ = -19\,900 + 44.8\,T \pm 5000$ [1093–1223 K]	This study
O (Y, 1 wt %) = O (Tb, 1 wt %) <sup>a</sup>	$\Delta G^\circ = 10\,900 + 13.9\,T \pm 4200$ [1093–1223 K]	This study
O (Y, 1 wt %) = O (Dy, 1 wt %) <sup>a</sup>	$\Delta G^\circ = 13\,400 + 10.4\,T \pm 3000$ [1093–1223 K]	This study
O (Y, 1 wt %) = O (Er, 1 wt %) <sup>a</sup>	$\Delta G^\circ = 38\,400 - 17.4\,T \pm 3900$ [1093–1223 K]	This study
O (Y, 1 wt %) = O (Ti, 1 wt %) <sup>a</sup>	$\Delta G^\circ = -50\,000 + 76.1\,T$ [1177–1438 K]	Okabe et al. [13]
1/2 O <sub>2</sub> (g) = O (Gd, 1 wt %) <sup>a</sup>	$\Delta G^\circ_{1,\text{Gd}} = -622\,000 + 109.8\,T \pm 5100$ [1093–1223 K]	This study
1/2 O <sub>2</sub> (g) = O (Tb, 1 wt %) <sup>a</sup>	$\Delta G^\circ_{1,\text{Tb}} = -591\,000 + 78.9\,T \pm 4600$ [1093–1223 K]	This study
1/2 O <sub>2</sub> (g) = O (Dy, 1 wt %) <sup>a</sup>	$\Delta G^\circ_{1,\text{Dy}} = -589\,000 + 75.4\,T \pm 2900$ [1093–1223 K]	This study
1/2 O <sub>2</sub> (g) = O (Er, 1 wt %) <sup>a</sup>	$\Delta G^\circ_{1,\text{Er}} = -564\,000 + 47.6\,T \pm 3700$ [1093–1223 K]	This study
1/2 O <sub>2</sub> (g) = O (Y, 1 wt %) <sup>a</sup>	$\Delta G^\circ_7 = -533\,000 + 12.4\,T$ [1177–1438 K] $\Delta G^\circ_7 = -602\,000 + 65.0\,T^b$	Okabe et al., experimental [13] Okabe et al. [13], calculated from $\Delta G^\circ_{f(\text{Y}_2\text{O}_3)}$ [4] and solubility data [6]
1/2 O <sub>2</sub> (g) = O (Ti, 1 wt %) <sup>a</sup>	$\Delta G^\circ_9 = -583\,000 + 88.5\,T^b$ [1173–1373 K] $\Delta G^\circ_9 = -562\,000 + 91.6\,T$ [1323–1573 K]	Okabe et al. [16] Niiyama et al. [17]
2/3Gd(s) + 1/2O <sub>2</sub> (g) = 1/3Gd <sub>2</sub> O <sub>3</sub> (s)	$\Delta G^\circ_{f(\text{Gd}_2\text{O}_3)} = -605\,000 + 92.3\,T$ [900–1300 K]	Barin [4]
2/3Tb(s) + 1/2O <sub>2</sub> (g) = 1/3Tb <sub>2</sub> O <sub>3</sub> (s)	$\Delta G^\circ_{f(\text{Tb}_2\text{O}_3)} = -616\,000 + 90.5\,T$ [900–1300 K]	Barin [4]
2/3Dy(s) + 1/2O <sub>2</sub> (g) = 1/3Dy <sub>2</sub> O <sub>3</sub> (s)	$\Delta G^\circ_{f(\text{Dy}_2\text{O}_3)} = -614\,000 + 90.7\,T$ [900–1300 K]	Barin [4]
2/3Er(s) + 1/2O <sub>2</sub> (g) = 1/3Er <sub>2</sub> O <sub>3</sub> (s)	$\Delta G^\circ_{f(\text{Er}_2\text{O}_3)} = -629\,000 + 93.1\,T$ [900–1300 K]	Barin [4]
2/3Y(s) + 1/2O <sub>2</sub> (g) = 1/3Y <sub>2</sub> O <sub>3</sub> (s)	$\Delta G^\circ_{f(\text{Y}_2\text{O}_3)} = -631\,000 + 92.4\,T$ [900–1300 K]	Barin [4]
Ca(l) + 1/2O <sub>2</sub> (g) = CaO (s)	$\Delta G^\circ_{f(\text{CaO})} = -637\,000 + 106\,T$ [1115–1300 K]	Barin [4]

<sup>a</sup> Oxygen activity in the RE–O solid solution is taken relative to an ultimately dilute standard state in which activity is equal to its 1 wt %. Dissolved oxygen is assumed to obey Sievert's law up to saturation.

<sup>b</sup> Selected reference data.

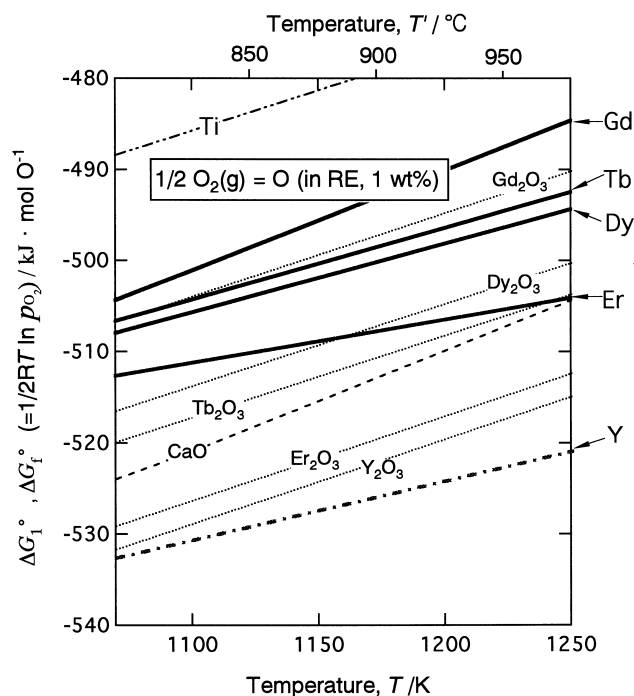


Fig. 6. Temperature dependence of the standard Gibbs energy change for oxygen dissolution,  $\Delta G_1^\circ$ , in rare earth metals obtained in this study. The standard Gibbs energy of formation of selected oxides,  $\Delta G_f^\circ$ , are also shown for comparison.

Y<sub>2</sub>O<sub>3</sub>, and CaO. For the solution of oxygen in RE metals, the Gibbs energy change becomes progressively more negative with increasing atomic number. Stability of sesquioxides also generally exhibits the same tendency, except that Tb<sub>2</sub>O<sub>3</sub> is more stable than Dy<sub>2</sub>O<sub>3</sub>. The figure shows that rare earth metals (RE=Gd, Tb, Dy, Er) containing 1 wt % oxygen can be deoxidized either by calcium or yttrium metal.

Kamihira et al. [19] have estimated the deoxidation limit of rare-earth metals by using the standard Gibbs energy of formation of the oxides because there was no information on the Gibbs energy of solution of oxygen at that time. From the data on RE–O solid solutions obtained in this study, it is possible to make more accurate estimate of the deoxidation limit using the various techniques. Recently, an electrochemical technique involving a molten salt, which can establish  $p_{\text{O}_2} = 10^{-49}$  atm at 1223 K [20] has been used for deoxidation of titanium and yttrium. Based on the Sievert's law consistent obtained in this study, it is estimated that the electrochemical technique can deoxidize Dy, Tb, Pr, and Er to 2, 4, 5 and 12 mass ppm, respectively.

There is no information in the literature on the saturation solubility of oxygen in RE metals. By assuming that Sievert's law is obeyed up to saturation, it is possible to estimate the solubility limit for oxygen in RE metals as a function of temperature. The oxygen partial pressure at saturation (RE/RE<sub>2</sub>O<sub>3</sub> two-phase field) can be calculated from thermodynamic data on oxides [4,21]. However, in view of the uncertainties in the data and possible devia-

tions from Sievert's law at high solute concentrations, it may be better to directly measure the saturation solubility by equilibration of the RE/RE<sub>2</sub>O<sub>3</sub> mixture with RE metal via the fused salt.

## 6. Conclusions

The distribution of oxygen between rare-earth metals (RE=Gd, Tb, Dy, Er) and yttrium and titanium reference metals were measured at temperatures between 1093 and 1233 K by equilibrating samples via a molten salt containing oxygen ions. The metal samples were submerged in calcium-saturated CaCl<sub>2</sub> melt containing a small quantity of dissolved CaO. The oxygen potential of the fused salt reservoir is controlled by the amount of dissolved CaO. The results were cross-checked by employing Y/Y<sub>2</sub>O<sub>3</sub> equilibrium to fix the oxygen potential.

The Gibbs energy change accompanying the solution of the oxygen in the rare-earth metals (RE=Gd, Tb, Dy, Er) has been obtained as a function of temperature. At 1173 K, the values for the Gibbs energy change in kJ mol<sup>-1</sup> for the reaction 1/2 O<sub>2</sub> (g)=O (RE, 1 wt % standard state), is obtained as -493 for Gd, -499 for Tb, -500 for Dy, and -508 for Er, respectively. It was found that the oxygen affinity of the metals decreases in the order Y>Er>Dy>Tb>Gd>Ti. For rare-earth metals, the Gibbs energy dissolution of oxygen becomes more negative with increasing atomic number. From the thermodynamic data obtained in this study it is estimated that the oxygen content the rare-earth metals can be brought down to the 10 ppm level by electrochemical deoxidation using a fused salt.

## Acknowledgements

The authors are indebted to Mr. H.Tokui (Shin-etsu Chemical Co. Ltd.) for preparation of high purity rare earth samples. This work was financially supported by Sasagawa Scientific Research Grant from the Japan Science Society, and partly funded by a Grant-in-Aid for Scientific Re-

search from the Ministry of Education, Science and Culture of Japan (No.08750851), and NEDO research grant (Project ID: 97S27003).

## References

- [1] K.A. Gschneider Jr., *J. Alloys Comp.* 193 (1993) 1.
- [2] C.K. Gupta, N. Krishnamurthy, *Int. Mater. Rev.* 37 (1992) 197.
- [3] Y. Shindo, H. Miyazaki, *Proc. Fall Meeting of MMIJ (Mining and Materials Processing Institute of Japan)*, Sapporo, 1992, p. 46.
- [4] I. Barin, *Thermochemical Data of Pure Substances*, VCH, Weinheim, 1989.
- [5] T.B. Massalski (Ed.), *Binary Alloy Phase Diagrams*, American Society for Metals, Metals Park, OH, 1990.
- [6] O.N. Carlson, R.R. Lichtenberg, J.C. Warner, *J. Less-Common Met.* 35 (1974) 275.
- [7] K. Kuroda, S. Takai, T. Fujisawa, M. Okido, C. Yamauchi, *Shigen-to-Sozai* 112 (1996) 893.
- [8] T.H. Okabe, R.O. Suzuki, T. Oishi, K. Ono, *Tetsu-to-Hagane* 77 (1991) 93.
- [9] T.H. Okabe, T. Oishi, K. Ono, *J. Alloys Comp.* 184 (1992) 43.
- [10] T.H. Okabe, T. Oishi, K. Ono, *Metall. Trans. B.* 23B (1992) 583.
- [11] T.H. Okabe, M. Nakamura, T. Oishi, K. Ono, *Metall. Trans. B.* 24B (1993) 449.
- [12] T.H. Okabe, T.N. Deura, T. Oishi, K. Ono, D.R. Sadoway, *J. Alloys Comp.* 237 (1996) 155.
- [13] T.H. Okabe, T.N. Deura, T. Oishi, K. Ono, D.R. Sadoway, *Metall. Trans. B.* 27B (1996) 841.
- [14] O. Kubaschewski, W.A. Dench, *J. Inst. Metals*, 82 (1953–54) 87.
- [15] K. Ono, S. Miyazaki, *J. Jpn. Inst. Metals* 49 (1985) 871.
- [16] T.H. Okabe, R.O. Suzuki, T. Oishi, K. Ono, *Mater. Trans.* 32 (1991) 485.
- [17] H. Niiyama, Y. Tajima, F. Tsukihashi, N. Sano, *J. Less-Common Met.* 169 (1991) 209.
- [18] O. Madelung (Ed.), *Landolt–Börnstein Numerical Data and Functional Relationships in Science and Technology*, vol. 26, Diffusion in Solid Metals and Alloys, Springer-Verlag, Berlin, 1982.
- [19] K. Kamihira, Y. Hasegawa, O. Ogawa, *Mater. Trans. JIM.* 34 (1993) 243.
- [20] K. Hirota, T.H. Okabe, E. Kasai, F. Saito, Y. Waseda, *Proc. Fall Meeting of MMIJ (Mining and Materials Processing Institute of Japan)* Sapporo, 6, 1997, p. 6.
- [21] M.W. Chase, J.L. Curnutt, H. Prophet, R.A. McDonald, A.N. Syverrud, *J. Phys. Chem. Ref. Data, JANAF Thermochemical Tables*, vol. 4, Supplement, American Chemical Society and American Institute of Physics, 1985.